Materials Science & Engineering A 639 (2015) 269–273

Contents lists available at ScienceDirect

Materials Science & Engineering A

journal homepage: www.elsevier.com/locate/msea

Rapid communication

# Fabrication of Ti–$Al_3Ti$ core–shell structured particle reinforced Al based composite with promising mechanical properties

Baisong Guo [a], Song Ni [a,b], Rujuan Shen [a], Min Song [a,b,*]

[a] State Key Laboratory of Powder Metallurgy, Central South University, Changsha 410083, China
[b] Institute for Materials Microstructure, Central South University, Changsha 410083, China

ARTICLE INFO

*Article history:*
Received 26 March 2015
Received in revised form
6 May 2015
Accepted 6 May 2015
Available online 15 May 2015

*Keywords:*
Aluminum matrix composite
Ti
$Al_3Ti$
Core–shell structure

ABSTRACT

In this paper, a Ti–$Al_3Ti$ core–shell structured particle reinforced pure Al based composite was fabricated by powder metallurgy technique. The composite has high compressive strength and ductility since the interface is clean and tight, and the propagation of the nucleated cracks in the shell during deformation can be effectively inhibited by soft Al matrix and Ti core. Although the residue pores and voids readily develop into large-sized pores in the matrix under tension, the composite still shows promising tensile mechanical properties.

## 1. Introduction

Particulate reinforced aluminum matrix composites (PRAMCs) have potential applications in automobile, chemical and aerospace industries due to their excellent mechanical properties such as low density, high strength and adjustable elastic modulus [1,2]. However, the addition of reinforcements (normally ceramic particles or intermetallics) in aluminum matrix decreases substantially the ductility and toughness. The degradation of the ductility and toughness results from two possible reasons. Firstly, if the interfacial bonding strength between the matrix and the reinforcements is weak, cracks can be easily nucleated along the interface during deformation [3–5]. Secondly, even if the interfacial bonding strength is strong, the brittle ceramic or intermetallic particles will fracture once the externally applied stress reaches a critical value [6–13]. Recently, we developed a new type of composite reinforced by Fe–$Al_xFe_y$ core–shell structured particles [12,14]. The reinforcements were formed in Al matrix by solid state reaction between pure Fe and Al powders during sintering process [12,14]. The composites with these special core–shell structured reinforcements have both high strength and compressive ductility (up to ~40%), compared to some composites reinforced by ceramic particles [14]. However, the tensile ductility was extremely low (less than 1%) due to the existence of pores or voids in the composites. The pores and voids were formed due to the volume expansion during phase transformation and exothermic reaction between Al and Fe powders during the sintering process.

In this paper, to further improve the ductility of the new composite, we substitute Fe by Ti to fabricate Ti–$Al_3Ti$ core–shell structured particle reinforced Al based composite using the same method. Compared to most Al-rich intermetallics, $Al_3Ti$ is very attractive because it has a high melting point (1623 K) and Young's modulus (~216 GPa), and low density (3.4 g/cm$^3$) [15]. In addition, Ti has low diffusivity and solubility in Al, hence $Al_3Ti$ can be expected to exhibit a low coarsening rate at elevated temperature [15,16]. Most important, the volume change and the heat release during the formation of $Al_3Ti$ are relatively low, which can help fabricate the composite with high density and less pores [17,18].

## 2. Experimental

The raw materials were gas atomized Al powder (99.8% in purity and average size of 2 μm) and commercial Ti powder (99.5% in purity and average size of 40 μm), with the volume fraction of the Ti powder being 10%. The mixed Al and Ti powders, combined with pure ethanol as the liquid medium, were ball-milled for 5 h in a 4 planetary ball mill under an argon atmosphere with a rotation speed of 300 rpm. The ball to powder weight ratio was 5:1. Then the mixed powders were dried in a vacuum oven at 75 °C for 5 h and die-pressed at room temperature under a pressure of 400 MPa in a cylindrical steel die with a diameter of 50 mm.

---

[*] Corresponding author at: State Key Laboratory of Powder Metallurgy, Central South University, Changsha 410083, China.
*E-mail address:* msong@csu.edu.cn (M. Song).

http://dx.doi.org/10.1016/j.msea.2015.05.015
0921-5093/

Subsequently, the compacts were compressed under an isostatic pressure of 150 MPa for 10 min to enhance the density. The green compacts were hot pressed using a graphite die at 660 °C for 5 h and then at 630 °C for 5 h with a pressure of 10 MPa under an argon atmosphere. The bulk density of the composite was measured by the standard Archimedes method. The strength and ductility of the composites were measured by both compressive and tensile testing methods. The compressive properties of the cylindrical samples, with diameter of 3 mm and height of 5 mm, were tested using an Instron 3369 universal testing machine with a strain rate of $3.3\times10^{-3}\,s^{-1}$ (cross head speed of 1 mm/min). The tensile specimens have been machined by wire-electrode cutting with a cross-section of $4\times3\,mm^2$ and a gauge length of 8 mm. The tensile tests were also carried out using the Instron 3369 testing machine with a strain rate of $2.1\times10^{-3}\,s^{-1}$ (cross head speed of 1 mm/min). The yield strength was determined as the 0.2 pct offset. The D/max2550pc X-ray diffractometer with Cu Kα radiation ($k$=0.154 nm) was applied to identify the phases in the composite. The microstructures of the composite were studied using an FEI Nova Nano230 scanning electron microscope (SEM) equipped with an energy dispersive spectroscopy (EDS) and a Titan G2 60-300 transmission electron microscope (TEM). Focus ion beam (FIB) was used to prepare the TEM samples.

## 3. Results and discussion

Fig. 1a shows an X-ray diffraction (XRD) pattern of the sintered sample. It can be seen that the composite has three phases, including Al, Ti and $Al_3Ti$. Fig. 1b shows an SEM image of the composite, showing that a lot of core–shell structured particles distribute uniformly in the Al matrix. Fig. 1c shows an enlarged SEM image and the corresponding EDS analysis. It can be seen that the composite consists of three different phases, including dark matrix, white core and gray shell. The EDS results reveal that the dark matrix is pure Al, the white core is pure Ti, and the gray shell is composed of ~71 at% Al and ~29 at% Ti, indicating that the shell is in situ formed intermetallic compound $Al_3Ti$. The relative density of the composite is 95.7%, which is higher than that of the Fe–$Al_xFe_y$ core–shell structured particle reinforced composite (~92.8%) fabricated using the same method [14]. However, it can be seen from Fig. 1c that a few small sized pores still exist in the intermetallic layer close to the Al side and Al matrix (indicated by black and white arrows, respectively). The pores in the intermetallic layer are due to the fact that Ti atoms diffuse faster than Al atoms during the sintering process, a phenomenon called the Kirkendall effect. Due to the faster Ti diffusion, not all sites are occupied by the flow of Al atoms from opposite direction and, therefore, there should be a flow of vacancies opposite to the faster diffusing Ti to compensate for the difference between the Ti and Al flux. Vacancies will then flow towards the Ti side while Ti will diffuse towards the Al-side, which results in the interface moving toward the Ti-rich side and away from the Al-rich side. If there is not enough plastic relaxation during the process, vacancies will coalesce to form pores or voids in the reaction layer [19–22]. The cavities in the matrix might be caused by the oxide layer of Al particles and the original pores in the green compact. The oxide layer can substantially degrade the solid-phase-sintering ability

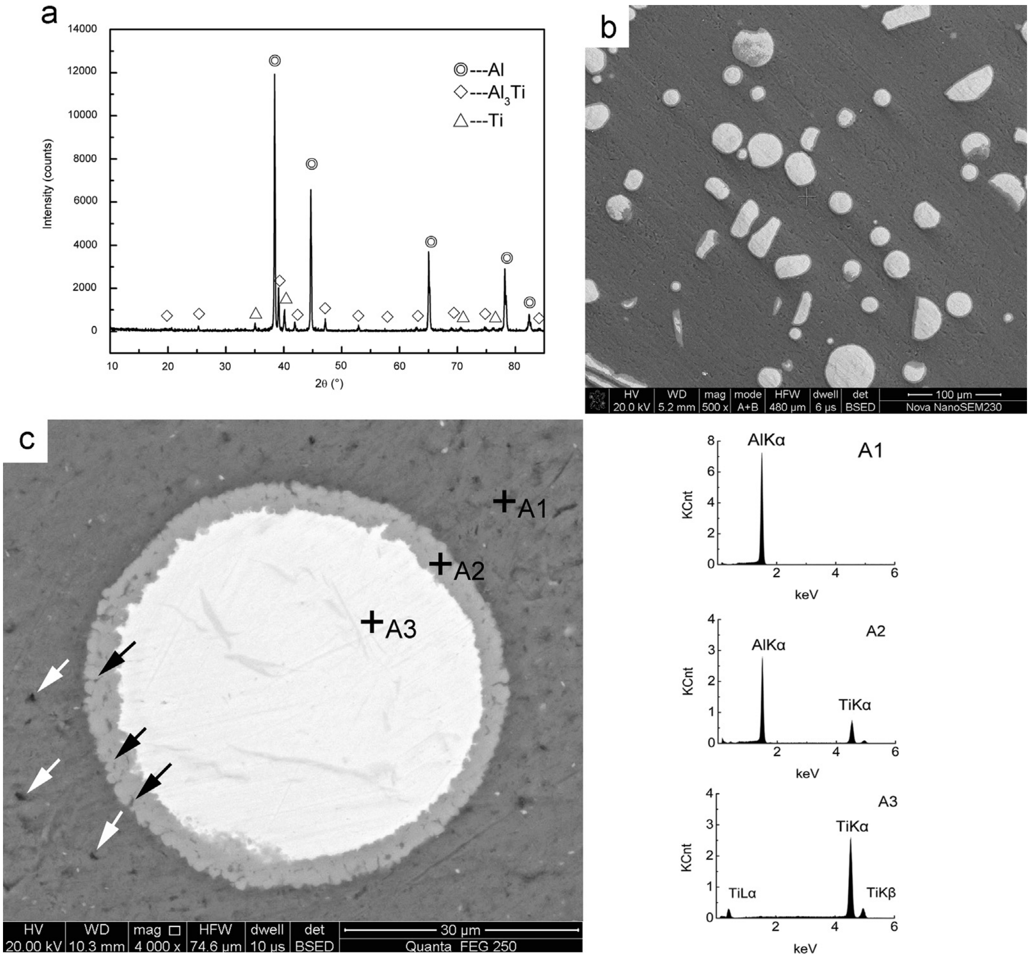

**Fig. 1.** (a) X-ray diffraction pattern, (b) back scattered SEM image and (c) enlarged SEM view and EDS analysis of the composite.